TNF activation of NF-κB is essential for development of single-positive thymocytes

Louise V. Webb,[1] Steven C. Ley,[2] and Benedict Seddon[1]

[1]Institute of Immunity and Transplantation, Division of Infection and Immunity, University College London, Royal Free Hospital, Rowland Hill Street, London NW3 2PF, England, UK
[2]Francis Crick Institute, Mill Hill Laboratories, London NW7 1AA, England, UK

NF-κB activation has been implicated at multiple stages of thymic development of T cells, during which it is thought to mediate developmental signals originating from the T cell receptor (TCR). However, the Card11–Bcl10–Malt1 (CBM) complex that is essential for TCR activation of NF-κB in peripheral T cells is not required for thymocyte development. It has remained unclear whether the TCR activates NF-κB independent of the CBM complex in thymocyte development or whether another NF-κB activating receptor is involved. In the present study, we generated mice in which T cells lacked expression of both catalytic subunits of the inhibitor of κB kinase (IKK) complex, IKK1 and IKK2, to investigate this question. Although early stages of T cell development were unperturbed, maturation of CD4 and CD8 single-positive (SP) thymocytes was blocked in mice lacking IKK1/2 in the T cell lineage. We found that IKK1/2-deficient thymocytes were specifically sensitized to TNF-induced cell death in vitro. Furthermore, the block in thymocyte development in IKK1/2-deficient mice could be rescued by blocking TNF with anti-TNF mAb or by ablation of TNFRI expression. These experiments reveal an essential role for TNF activation of NF-κB to promote the survival and development of single positive T cells in the thymus.

The Journal of Experimental Medicine

CD4 and CD8 lineage T cells develop in the thymus through a series of complex selection events evolved to identify those thymocytes with self-MHC–restricted TCRs and direct their development to the appropriate subset. There has been considerable interest in defining the signaling pathways and transcriptional networks responsible for controlling T cell development. NF-κB transcription factors regulate the survival, function, and development of many cell types, including those of the immune system (Bonizzi and Karin, 2004). Canonical NF-κB signaling is mediated by the inhibitor of κ B kinase (IKK) complex, comprised of two catalytic subunits, IKK1 (IKKα) and IKK2 (IKKβ), and a regulatory ubiquitin-binding adaptor, NEMO (IKKγ). Phosphorylation by the IKK complex targets inhibitor of κ Bα (IκBα) for degradation by the proteasome, releasing associated NF-κB1 p50/Rel and NF-κB1 p50/cRel dimers to enter the nucleus and stimulate gene transcription.

NF-κB has been shown to control T cell development at various checkpoints. Inhibition of NF-κB activity by T cell expression of a degradation-resistant IκBα super-repressor blocks the CD4 CD8 double-negative (DN) to CD4 CD8 double-positive (DP) transition, suggesting a role for NF-κB downstream of the pre-TCR complex in DN thymocytes (Voll et al., 2000). Super-repressor IκBα expression has also be reported to inhibit positive selection of CD8 SP thymocytes, which have the highest level of detectable NF-κB activity in the thymus (Mora et al., 1999; Hettmann and Leiden, 2000). Consistent with this, transgenic expression of a constitutively active IKK2 mutant to increase NF-κB in T cells enhances CD8 SP development (Jimi et al., 2008). Because TCR signals regulate TCRβ selection in DN thymocytes, and positive and negative selection at the DP stages, it is thought that the observed functions of NF-κB are the result of TCR-dependent triggering. However, TCR activation of the IKK complex in peripheral T cells is mediated via a complex comprising Card11, Bcl10, and Malt1 proteins (the CBM complex) that is not required for thymocyte development (Schmidt-Supprian et al., 2004). This implies that the TCR in thymocytes stimulates IKK independently of the CBM complex or that another receptor is responsible for activating NF-κB in these cells.

In the present study, we reinvestigated the role of NF-κB in thymocyte development using mice in which both *Ikk1* and *Ikk2* genes had been deleted in early thymic progenitors (IKKΔT). Thymic development was completely arrested at the HSA^{hi} SP stage. In vitro experiments demonstrated that blockade of NF-κB activation specifically sensitized thymocytes to TNF-induced cell death. In line with this, inhibiting TNF signaling with an antibody or deletion of TNFRI rescued the development of SP thymocytes in IKKΔT mice. These results reveal a critical role for TNF in the development of SP T cells in the thymus.

Correspondence to Benedict Seddon: benedict.seddon@ucl.ac.uk

Abbreviations used: CBM, Card11–Bcl10–Malt1; DN, double negative; DP, double positive; IAP, inhibitor of apoptosis; IKK, inhibitor of κ-B kinase; SP, single positive.

The Rockefeller University Press $30.00
J. Exp. Med. 2016 Vol. 213 No. 8 1399–1407
www.jem.org/cgi/doi/10.1084/jem.20151604

RESULTS AND DISCUSSION

NF-κB signaling is redundant for development and selection of DP thymocytes, but essential for SP thymocyte maturation

To investigate the role of NF-κB signaling in thymocyte development, we used the Cre-Lox system to delete conditional alleles of *Ikk1* and *Ikk2* genes within the T cell lineage. Previous studies show that thymic development proceeds relatively normally in the absence of either *Ikk1* or *Ikk2* expression (Schmidt-Supprian et al., 2003; Chen et al., 2015), even when gene deletion occurs early in T cell development in DN2 thymocytes (Silva et al., 2014), with the exception of thymic regulatory T cell development that is reduced by lack of either IKK1 or IKK2. This suggests that there is significant redundancy between these two subunits for activating IKK activity and canonical NF-κB signaling. Therefore, to achieve a complete block in IKK function, we generated $Ikk1^{fx/fx}$ $Ikk2^{fx/fx}$ mice to delete both kinase subunits, using either $huCD2^{iCre}$ to delete in DN2 thymocytes ($IKK\Delta T^{CD2}$) or $CD4^{Cre}$ to delete in DP thymocytes ($IKK\Delta T^{CD4}$). Cre activity was monitored by the inclusion of $Rosa26^{RYFP}$ reporter alleles (Srinivas et al., 2001). Surprisingly, early deletion of IKK genes by $huCD2^{iCre}$ did not result in any obvious defects in DN or DP development. Number and representation of DN3 and DN4 thymocytes were not obviously perturbed in $IKK\Delta T^{CD2}$ mice (Fig. 1 A). Similarly, subsets of DP thymocytes defined by expression of TCR and CD5 (Saini et al., 2010) were normally represented (Fig. 1 B). In contrast, the TCR^{hi} SP compartment was profoundly affected. Percentages of both CD4SP and CD8SP were reduced (Fig. 1 C) and analysis of cell phenotype revealed that mature HSA^{lo} SPs were greatly reduced in number in the absence of *Ikk* genes (Fig. 1 C). This block in development was also evident in $IKK\Delta T^{CD4}$ mice in which gene deletion occurred at the DP stage (Fig. 1 D). In the periphery, there was a corresponding reduction in the naive T cell compartment in $IKK\Delta T^{CD2}$ mice compared with controls (Fig. 1 E). The few naive, memory, and regulatory cells present (Fig. 1 E) were largely Cre reporter YFP-negative (Fig. 1 F) and therefore most likely represent escapants, in which *Ikk1* and/or *Ikk2* gene deletion was incomplete. Together, these data demonstrate a critical role for IKK1/2 in the development of SP thymocytes, whereas earlier stages of thymocyte development are IKK1/2-independent. These results are consistent with earlier reports on the effects of Nemo deficiency upon development of SP thymocytes (Schmidt-Supprian et al., 2003).

IKK1/2-deficient thymocytes are specifically sensitive to TNF-induced apoptosis

We next investigated which receptors might be responsible for triggering the NF-κB activation required for SP thymocyte development, other than TCR. TNF receptor superfamily (Tnfrsf) members are potent activators of NF-κB, and those receptors with death domains can also recruit the adapter TRADD and/or FADD to trigger caspase-induced cellular

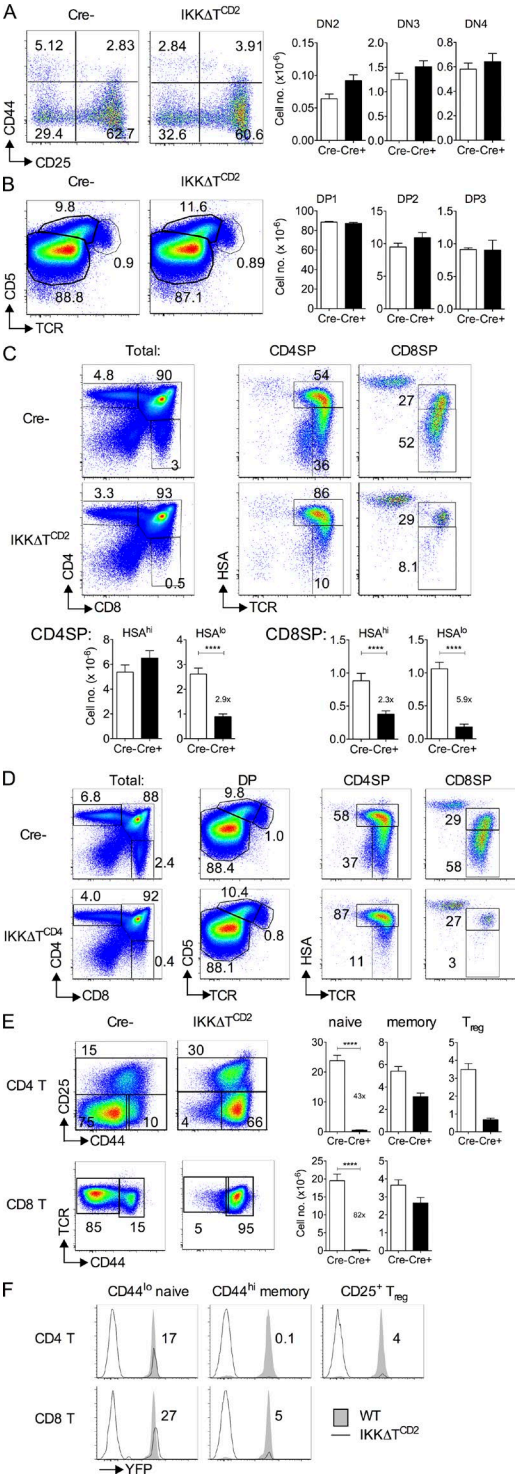

Figure 1. **Deletion of *Ikk1* and *Ikk2* blocks SP thymocyte development.** Lymphoid organs from 8–12-wk-old $Ikk1^{fx/fx}$ $Ikk2^{fx/fx}$ $R26^{REYFP}$ $huCD2^{iCre}$ ($IKK\Delta T^{CD2}$, $n = 16$) were analyzed by FACS and compared with $huCD2^{iCre}$ -ve (Cre^-, $n = 15$) littermate as control. (A) Density plots are of CD44 versus CD25 by DN Lin^- (CD4, CD8, TCRαβ, and CD5) thymocytes. Numbers indicate percentage in the corresponding quadrant. Bar charts are cell number of $CD44^{hi}CD25^{hi}$ (DN2), $CD44^{lo}CD25^{hi}$ (DN3), and $CD44^{lo}$

apoptosis or necroptosis (Vandenabeele et al., 2010). One possible role for NF-κB in developing thymocytes could be to prevent induction of cell death induced by such receptors.

Our previous studies reveal that SP thymocytes express *Tnfrsf* members TNF receptor I and II, CD27 (*Tnfrsf7*), TACI (*Tnfrsf13b*), LIGHTR (*Tnfrsf14*), GITR (*Tnfrsf18*), *Tnfrsf25*, and *Tnfrsf26* (Silva et al., 2014). We therefore asked whether ligands for these receptors could induce apoptosis in IKK1/2-deficient thymocytes, which could account for the phenotype of IKKΔT mice. Thymocytes from IKKΔT^{CD4} mice were cultured overnight with TNF (ligand for TnfrI and TnfrII), CD27L, APRIL, or BAFF (TACI ligands), LIGHT (LIGHTR ligand), TRAIL (ligand for Tnfrsf26), GITRL (GITR ligand), or TL1A (ligand for DR3/Tnfrsf25), and then viability assessed. Thymocyte survival was unaffected by all ligands except TNF which induced a substantial increase in cell death in SP thymocytes (Fig. 2 A). To examine this in more detail, we measured TNF-induced cell death on different thymic subsets from IKKΔT^{CD4} mice, as well as WT and *Tnfrsf1a*$^{-/-}$ donors as controls. TNF promoted cell death in a small fraction of DP and HSA^{hi} CD4SP subsets from both WT and IKKΔT^{CD4} donors. In contrast, TNF stimulation had no effect upon cell viability of HSA^{lo} CD4SP or either CD8SP subset from WT mice, but induced high levels of cell death in the same populations from IKKΔT^{CD4} mice (Fig. 2 B). The viability of thymocytes from *Tnfrsf1a*$^{-/-}$ mice was unaffected by TNF, confirming that TNFRI was required to transmit proapoptotic TNF signals in DP and HSA^{hi} CD4 SP.

The few SP cells that developed in IKKΔT^{CD4} mice were highly sensitive to TNF-induced cell death in vitro, consistent with earlier studies that IKK2-deficient T cells are sensitive to TNF-induced cell death (Senftleben et al., 2001). However, development of IKK2-deficient thymocytes is normal (Schmidt-Supprian et al., 2003; Silva et al., 2014), in contrast to that of IKKΔT mice. Because IKKΔT cells had developed in the absence of IKK1/2, it was unclear whether the sensitivity of SP cells to TNF reflected a normal requirement for IKK1/2 for their survival after TNF stimulation. To investigate this, we analyzed responses of thymocytes from huCD2^{iCre} *Ikk1*$^{fx/fx}$ mice cultured with IKK2-specific inhibitor Bl605906 (Clark et al., 2011). In the absence of IKK1 protein, IKK2 inhibition results in a near complete block in canonical NF-κB signaling (Clark et al., 2011). Importantly, thymic development in IKK1-deficient mice is grossly normal (Chen et al., 2015). Thymocytes from huCD2^{iCre} *Ikk1*$^{fx/fx}$ mice (lacking only IKK1) were resistant to TNF-induced cell death, similar to WT thymocytes. Only a small fraction of HSA^{hi} CD4SP were induced to die by TNF, whereas viability of all other SP subsets were unaffected by TNF (Fig. 2 C). However, culture with IKK2 inhibitor rendered HSA^{lo} CD4SP and both subsets of CD8SPs from huCD2^{iCre} *Ikk1*$^{fx/fx}$ mice profoundly susceptible to death induction by TNF (Fig. 2 C). TNF also induced active caspase 8 in cultures of huCD2^{iCre} *Ikk1*$^{fx/fx}$ thymocytes and IKK2 inhibitor, providing evidence that TNF induced apoptotic cell death. Together, these data suggest that TNF RI activation of IKK/NF-κB activity was required to protect thymocytes from TNF-induced apoptosis. The susceptibility of thymic subsets to TNF-induced apoptosis in vitro, as assessed by Bl605906 IC_{50} values (Fig. 2 E), mirrored the phenotype of IKK1/2-deficient thymocytes in vivo. HSA^{hi} CD4SPs were least susceptible to TNF-induced cell death in vitro and were minimally affected in IKKΔT^{CD4} mice. In contrast, HSA^{lo} CD8SP thymocytes were most sensitive to TNF-induced cell death in the absence of IKK activity and were virtually absent from IKKΔT^{CD4} mice.

Because the IKK complex is known to regulate cell function independently of NF-κB (Yan et al., 2013; Dondelinger et al., 2015), it was important to confirm that the effects of IKK1/2 deficiency on thymocyte development were actually due to reduced NF-κB activation. First, we confirmed that IKK2 blockade in IKK1-deficient thymocytes did indeed prevent NF-κB activation by TNF (Fig. 2 F). Second, we analyzed a transgenic mouse strain in which thymocytes express a dominant-negative inhibitor of κB (pLck-IκB-PEST), in which CD8SP development is significantly impaired (Mora et al., 1999). HSA^{lo} CD4SP, HSA^{hi} CD8SP, and HSA^{lo} CD8SP thymocytes from pLck-IκB-PEST mice were more susceptible to TNF-induced cell death, whereas HSA^{hi} CD4SP remained relatively unaffected by IκB-PEST expression compared with controls (Fig. 2 G). These results confirm that TNF activation of NF-κB is required for thymocyte survival in vitro.

CD25^{lo} (DN4) DN thymocyte subsets. (B) Density plots are of TCR versus CD5. Numbers indicate percentage in the corresponding gate. Bar charts are cell number of CD5^{lo}TCR^{lo} (DP1), CD5^{hi}TCR^{int} (DP2), and CD5^{int}TCR^{hi} (DP3) DP subsets. (C) Density plots are of CD4 versus CD8 expression by total live thymocytes and TCR versus HSA by CD4SP and CD8SP gated thymocytes. Bar charts show numbers of the indicated SP subset from IKKΔT^{CD2} mice (Cre^{+}) and huCD2^{iCre} -ve (Cre^{-}) littermates. Numbers indicate fold difference in counts between Cre^{-} and Cre^{+}. (D) Density plots are of CD4 versus CD8 expression by total live thymocytes, TCR versus CD5 by DP thymocytes, and TCR versus HSA by CD4SP and CD8SP gated thymocytes from IKKΔT^{CD4} mice or Cre^{-} littermates. (E) Density plots are CD25 versus CD44 by CD4^{+}TCR^{hi} gated lymph node cells and CD44 versus TCR by CD8^{+}TCR^{hi} gated lymph node cells from the indicated strains and show gates used to define naive (CD44^{lo} CD25^{-}), memory (CD44^{hi} CD25^{-}), and T reg (CD25^{+}) cells among CD4^{+}TCR^{hi} cells, and naive (CD44^{lo}) and memory (CD44^{hi}) among CD8^{+}TCR^{hi} cells. Bar charts show total number of naive, memory, and T reg cells recovered from lymph node and spleen of IKKΔT^{CD2} mice (Cre^{+}) and huCD2^{iCre} -ve (Cre^{-}) littermates. Numbers indicate fold difference in naive cell counts between Cre^{-} and Cre^{+} hosts. (F) Histograms are of EYFP expression by naive, memory, and regulatory CD4^{+}TCR^{hi} T cells and naive and memory CD8^{+}TCR^{hi} T cells from IKKΔT^{CD2} mice and huCD2^{iCre} *Ikk1*$^{fx/WT}$ *Ikk2*$^{fx/WT}$ *R26*^{REYFP} littermate controls (WT). Numbers indicate percentage of IKKΔT^{CD2} cells (solid lines) expressing YFP. FACS data are representative of four or more experiments and cell number data are pooled from four experiments. ****, $P < 0.0001$.

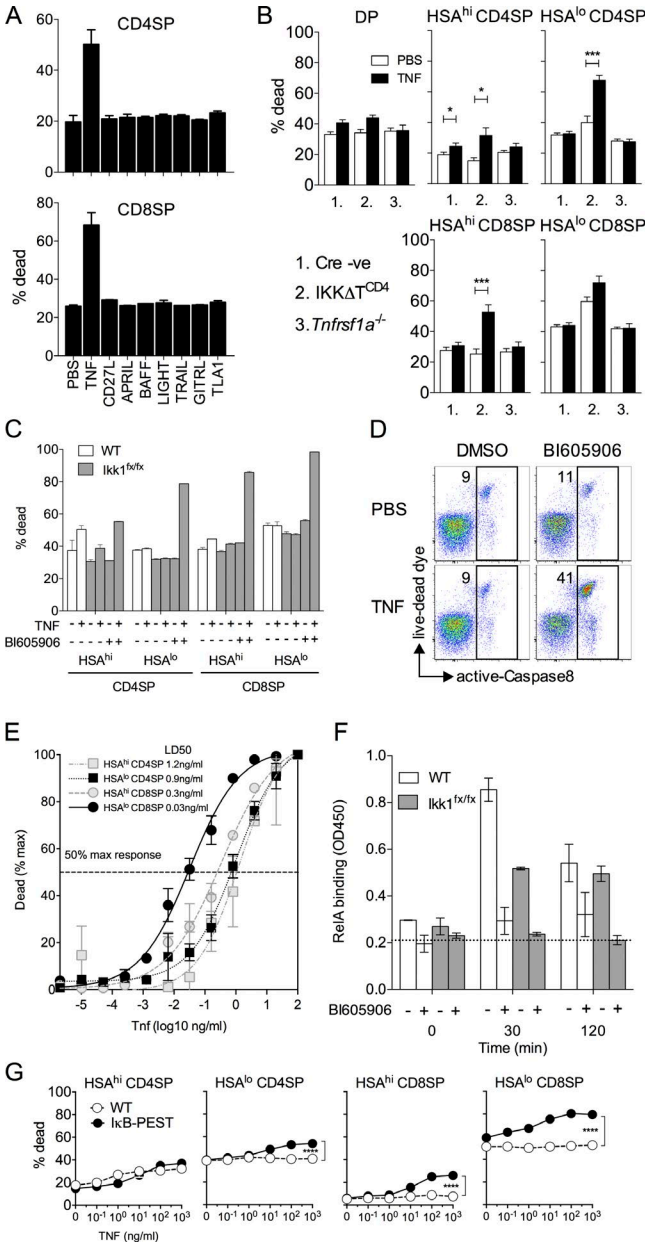

Figure 2. **TNF induces thymocyte cell death in the absence of IKK activity in vitro.** (A) Thymocytes from *Ikk1*$^{fx/fx}$ *Ikk2*$^{fx/fx}$ R26^{REYFP} CD4^{Cre} (IKKΔT^{CD4}) mice were cultured overnight with the indicated *Tnfrsf* member, and viability of the indicated SP subset assessed the next day by FACS. (B) Thymocytes from IKKΔT^{CD4}, Cre -ve littermates (Cre -ve), and *Tnfrsf1a*$^{-/-}$ donors were cultured overnight with and without TNF (30 ng/ml). Bar chart shows viability among the indicated subsets cultured with addition of PBS (open bars) or TNF (filled bars) as assessed by FACS. (C) Thymocytes from WT and *Ikk1*$^{fx/fx}$ *R26*^{REYFP} huCD2^{iCre} donors were cultured overnight in the presence of TNF or IKK2 inhibitor BI605906, or both. Bar chart shows percentage of viability among the indicated subsets as assessed by FACS. (D) *Ikk1*$^{fx/fx}$ *R26*^{REYFP} huCD2^{iCre} thymocytes were cultured for 4 h in the presence of TNF and/or IKK2 inhibitor BI605906. Density plots are of live dead versus active caspase 8 stain by CD8 SP thymocytes. (E) Thymocytes from *Ikk1*$^{fx/fx}$ *R26*^{REYFP} huCD2^{iCre} donors were cultured with IKK2 inhibitor and a titration of TNF. Line graph shows the percentage of maximum TNF-induced death for different concentrations of TNF, above background, for the indicated subsets. Concentrations in figure legend indicate LD_{50} of TNF for the corresponding subset. (F) Thymocytes from WT or *Ikk1*$^{fx/fx}$ *R26*^{REYFP} huCD2^{iCre} donors were pre-incubated with IKK2 inhibitor BI605906 or DMSO vehicle for 1 h where indicated, and then stimulated with TNF and nuclear extracts prepared at different times. Bar charts represent RelA binding to NF-κB binding oligonuclotides as detected by ELISA and displayed as OD. Dotted line indicates the background signal from blank wells. (G) Thymocytes from pLck-IκB-PEST donors or transgene -ve littermates were cultured in different concentrations of TNF overnight. Line graphs are of percentage dead cells in the indicated subsets from pLck-IκB-PEST donors (IκB-PEST, filled circles) or transgene negative litter controls (WT, open circles). Error bars indicate SD of technical duplicates. Data are representative of two (F), three (G), or more (A–E) independent experiments. *, $P < 0.05$; ***, $P < 0.001$.

Blockade of TNF signaling via TNFRI rescues IKKΔT SP thymocyte development

We next asked whether the susceptibility of SP thymocytes to TNF-induced cell death observed in vitro could account for the abnormal thymic development in mice with impaired NF-κB signaling. IKKΔT^{CD4} mice were treated with neutralizing anti-TNF mAb for 7 d. This short period of TNF blockade was sufficient to restore both HSA^{lo} CD4SP and total CD8SP thymic subsets in treated mice (Fig. 3 A). Examining T cells in lymph nodes of treated mice at day 7 revealed a significant increase in the number of naive T cells in anti-TNF–treated mice, suggesting that newly developing SP cells were also able to emigrate to the periphery (Fig. 3 B). To determine if TNF signaling was transmitted by TNFRI receptor, we additionally generated *Tnfrsf1a*$^{-/-}$ IKKΔT^{CD4} mice. Loss of TNFRI expression also restored development of mature SP subsets in IKKΔT^{CD4} mice (Fig. 3 C). Enumerating different subsets of thymocytes revealed that anti-TNF treatment resulted in comparable rescue of SP thymic development in IKKΔT^{CD4} mice to that in *Tnfrsf1a*$^{-/-}$ IKKΔT^{CD4} mice (Fig. 3 D).

Analyzing the periphery of *Tnfrsf1a*$^{-/-}$ IKKΔT^{CD4} mice revealed a substantial increase in numbers of naive T cells compared with IKKΔT^{CD4} controls (Fig. 3 E). However, repopulation was still only a fraction of that observed in Cre-WT controls. We have previously shown that NF-κB signaling is required for normal expression of IL-7Rα by naive T cells, which is necessary for their long-term survival (Silva et al., 2014). Naive T cells from *Tnfrsf1a*$^{-/-}$ IKKΔT^{CD4} mice displayed a substantial reduction in IL-7Rα levels compared with controls (Fig. 3 E). Impaired IL-7Rα expression therefore may explain why *Tnfrsf1* deletion in absence of IKK1/2 expression did not rescue naive T cell numbers more efficiently in the periphery.

Lastly, we asked whether the defect in CD8SP development reported in pLck IκB-PEST mice could also be corrected by anti-TNF treatment. Analyzing thymocytes from pLck-IκB-PEST mice revealed that the reduced abundance of CD8SP was a result of a specific reduction in HSA^{lo} CD8SP thymocytes (Fig. 4), that we also found to be most sensi-

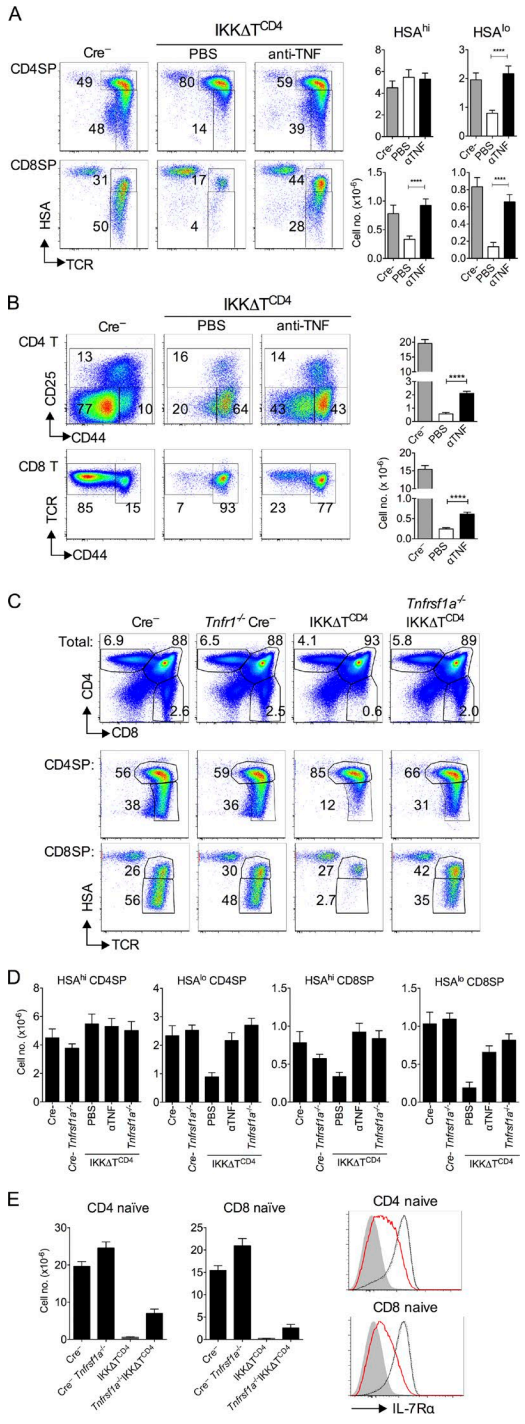

Figure 3. **TNF blockade rescues SP development in IKKΔT^{CD4} mice.** (A and B) *Ikk1*$^{fx/fx}$ *Ikk2*$^{fx/fx}$ R26^{REYFP} CD4^{Cre} (IKKΔT^{CD4}) mice (8–16 wk old) were treated with anti-TNF mAb i.p. (1 mg/inject; n = 16) or PBS as control (n = 17). After 7 d, thymus and lymph node cells were analyzed by FACS. (A) Density plots are of TCR versus HSA expression by CD4SP (top row) and CD8 SP (bottom row) from IKKΔT^{CD4} mice treated with anti-TNF or PBS as compared with untreated Cre -ve littermate controls (Cre$^-$, n = 17). Bar charts show total cell recoveries of HSA^{hi} and HSA^{lo} cells among CD4SP (top row) and CD8SP (bottom row). (B) Density plots are of CD44 versus CD25 by CD4$^+$TCR^{hi} T cells (top row) and CD44 versus TCR by CD8$^+$ cells from lymph nodes of the same treatment groups described in A. Bar charts show cell numbers of naive CD4 (top chart) and naive CD8 (bottom chart) T cells from mice. (C) Density plots are of CD4 versus CD8 by total live thymocytes (top row), and TCR versus HSA by CD4SP (middle row) and CD8SP thymocytes (bottom row) from IKKΔT^{CD4} mice, Cre -ve littermate controls (Cre$^-$), *Tnfrsf1a*$^{-/-}$ IKKΔT^{CD4} mice (n = 16), and Cre -ve littermate controls (*Tnfrsf1a*$^{-/-}$ Cre$^-$, n = 13). (D) Bar charts show cell numbers of the indicated SP subset recovered from IKKΔT^{CD4} mice treated with anti-TNF (αTNF) or PBS as described in A, untreated Cre -ve littermates (Cre$^-$), or *Tnfrsf1a*$^{-/-}$ IKKΔT^{CD4} mice and Cre -ve littermate controls (*Tnfrsf1a*$^{-/-}$ Cre$^-$). (E) Bar charts show total numbers of naive CD44^{lo} CD25$^-$ CD4$^+$ TCR^{hi} T cells and naive CD44^{lo} CD8$^+$ TCR^{hi} T cells from lymph nodes of *Ikk1*$^{fx/fx}$ *Ikk2*$^{fx/fx}$ R26^{REYFP} CD4^{Cre} (IKKΔT^{CD4}, n = 17) mice, Cre -ve littermates (Cre$^-$, n = 17), *Tnfrsf1a*$^{-/-}$ IKKΔT^{CD4} mice (n = 16), and Cre -ve littermate (Cre– *Tnfrsf1a*$^{-/-}$, n = 13) as control. Histograms are of IL-7Rα by gated naive CD44^{lo} CD25$^-$ CD4$^+$ TCR^{hi} T cells (top) and naive CD44^{lo} CD8$^+$ TCR^{hi} T cells (bottom) from WT (black broken lines), *Tnfrsf1a*$^{-/-}$ IKKΔT^{CD4} mice (red solid lines) and Cre -ve *Tnfrsf1a*$^{-/-}$ littermates (solid line). Gray fills are IL-7Rα expression by DP thymocytes from WT mice as negative control. FACS data are representative of four or more independent experiments, and bar charts are pooled from four or more independent experiments. ****, P < 0.0001.

tive to TNF-induced cell death in vitro (Fig. 2 E). Consistent with this, TNF blockade in these mice for 7 d resulted in restoration of normal HSA^{lo} CD8SP compartment (Fig. 4), suggesting that TNF-induced cell death accounted for the apparent skew in T cell development that had previously been interpreted as a block in selection of CD8 lineage cells.

An absence of TNF gene targets from IKK-deficient SP thymocytes

The mechanisms by which NF-κB activation protects cells from TNF-induced cell death have been intensively studied in a variety of cell types. Several NF-κB target genes have been identified that regulate cell survival after TNF stimulation, including cFLIP, Traf1, Traf2, and members of the inhibitors of apoptosis (IAP) family (Chu et al., 1997; Wang et al., 1998; Kreuz et al., 2001; Micheau et al., 2001; Turner et al., 2007). Conversely, NF-κB–induced expression of Cyld has been reported to provide negative feedback to TNFR signaling and NF-κB activation (Jono et al., 2004). Transcriptional profiling was used to investigate whether any of these NF-κB targets might regulate TNF-induced thymocyte survival. TCR transgenic CD8SP thymocytes were stimulated with TNF in vitro for 4 h and gene expression was determined by RNAseq. Analysis of gene expression revealed the induction of several classical NF-κB targets, such as NF-κB1, NF-κB2, inhibitor of κBa (*Nfkbia*), and Bcl3 (Haskill et al., 1991; Ten et al., 1992; Lombardi et al., 1995; Brocke-Heidrich et al., 2006), as well as other reported targets *Traf1* and *Il7r* (Schwenzer et al., 1999; Miller et al., 2014; Fig. 5 A). The prosurvival genes, *Cflar* (cFLIP) and *Xiap* were not induced by TNF stimulation of thymocytes. Levels of *Cyld* and *Diablo/SMAC* mRNAs were unaffected by TNF stimulation. In contrast, the expression of

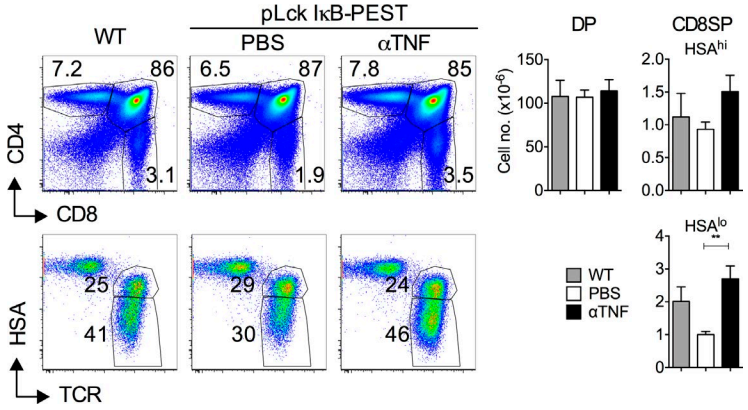

Figure 4. **TNF blockade rescues the developmental block in pLck IκB-PEST mice.** pLck IκB-PEST mice were treated with anti-TNF ($n = 8$; 1 mg, days 0, 2, and 4) or PBS ($n = 8$) injection as control. At day 7, thymi were analyzed by FACS. Density plots are of CD4 versus CD8 by total live (top row) and HSA versus TCR by CD8SP gated thymocytes from pLck IκB-PEST mice treated with either anti-TNF (αTNF) or PBS as control. Transgene -ve (WT, $n = 4$) littermates were also analyzed as control. Bar charts show total cell numbers of the indicated thymocyte subset recovered from the indicated treatment groups. Data are pooled from two independent experiments. **, $P < 0.01$.

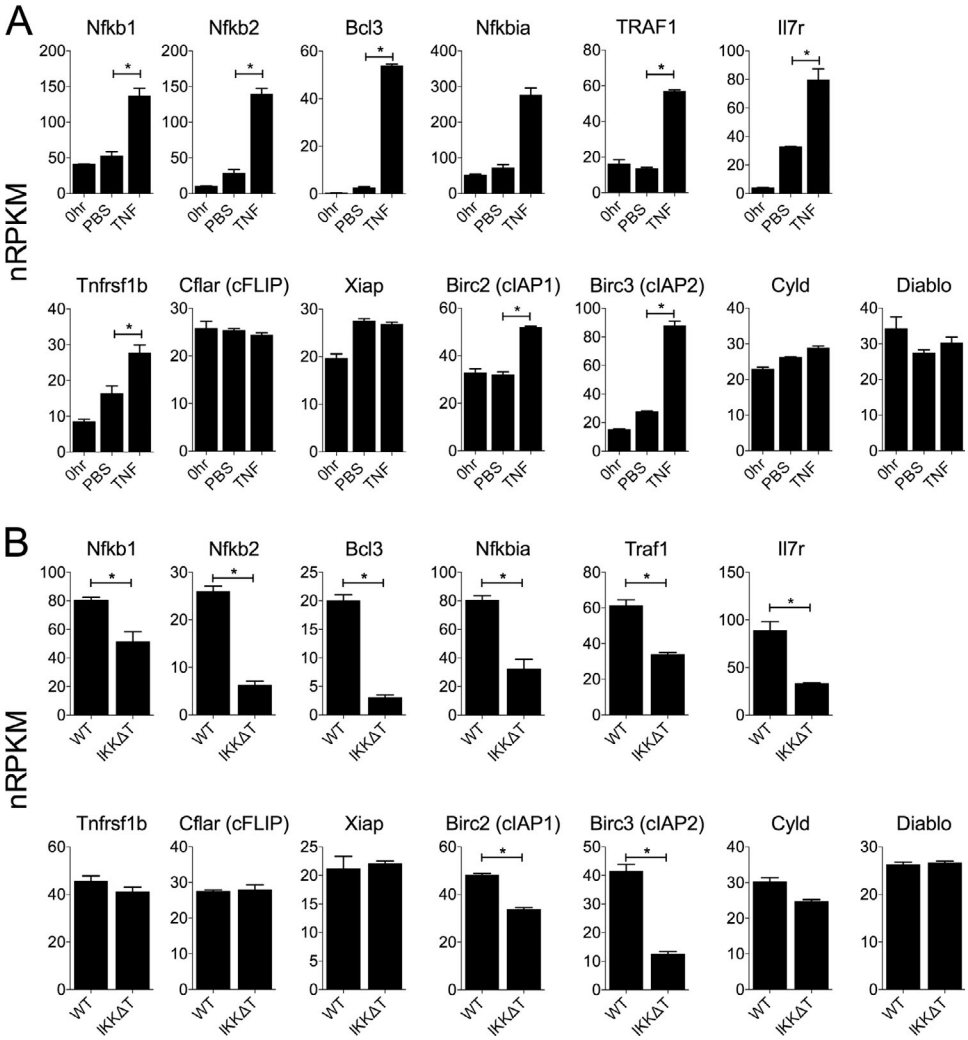

Figure 5. **cIAP1 and cIAP2 expression is induced by TNF in vitro and is NF-κB dependent in vivo.** (A) TCR^{hi} CD8SP thymocytes from F5 *Rag1*$^{-/-}$ donors were sort purified and stimulated with TNF ($n = 4$) or PBS ($n = 4$) as control. mRNA was isolated from cultured and uncultured cells (0 h, $n = 3$) and gene expression determined by RNAseq analysis. Bar charts show mRNA expression level (normalized reads per kb exons per million reads, nRPKM) of the indicated genes. Names in brackets indicate protein name associated with gene. (B) TCR^{hi} CD8SP thymocytes were sorted from WT ($n = 3$) and *Tnfrsf1a*$^{-/-}$ IKKΔT^{CD4} mice ($n = 4$). mRNA was purified and gene expression was determined by RNAseq analysis. Bar charts show mRNA expression level (nRPKM) of the indicated genes. Individual RNAseq libraries were generated from independent cell preparation and treatments. *, $P < 0.05$.

Birc3 (cIAP2) mRNA was strongly increased by TNF stimulation, and *Birc3* (cIAP2) mRNA to a lesser extent.

To test whether expression of any of these NF-κB target genes was reduced in IKK1/2-deficient thymocytes, we performed RNAseq on sorted CD8SP thymocytes from *Tnfrsf1a*$^{-/-}$ IKKΔT^{CD4} and control WT mice. Although TNFRII gene expression (Tnfrsf1b) was modestly induced by TNF in vitro, no modulation was observed in IKKΔT^{CD4} mice in vivo (Fig. 5), arguing against a role for modulated TNFRII levels in the rescue of development by TNF blockade. Significantly, those genes found to be positively regulated by TNF in vitro were all expressed at reduced levels in vivo in the absence of IKK1/2 (Fig. 5 B). Similarly, those potential NF-κB targets that were not regulated in vitro were also unaffected by IKK ablation in vivo (Fig. 5 B). Together, these data suggest that defective IAP2 and IAP1 expression sensitizes IKK1/2-deficient thymocytes to TNF-induced cell death.

Conclusion

The role of NF-κB signaling during development of conventional T cells has previously been almost exclusively considered in the context of TCR signaling. Our study identifies TNF as the key trigger of NF-κB activation required to promote thymocyte development. CD8 SP thymocytes were especially sensitive to TNF-induced cell death in the absence of NF-κB activation, and this likely accounts for the apparent selective defects in CD8 lineage development previously reported and attributed to altered TCR selection signaling.

We recently showed that *Il7r* is a NF-κB target gene necessary for long-term survival of peripheral naive T cells (Silva et al., 2014), and it seems likely that NF-κB regulates other gene targets necessary for normal T cell function. Our study also aligns development of conventional T cells with that of regulatory T cells, which rely upon the cooperative activity of several *Tnfrsf* members for their development (Mahmud et al., 2014). Determining whether TNFR cooperates with other *Tnfrsf* members and the role of NF-κB activation downstream of such receptors will be important areas for future studies.

MATERIALS AND METHODS

Mice. Mice with conditional alleles of Ikk2 (Ikk2$^{fx/fx}$; Li et al., 2003) and Ikk1 (Ikk1$^{fx/fx}$; Gareus et al., 2007) were intercrossed with mice either expressing transgenic Cre under the control of the human CD2 (huCD2; de Boer et al., 2003) or CD4 expression elements. Rosa26 reporter YFP allele (R26REYFP; Srinivas et al., 2001) was also used to facilitate identification of cells in which Cre recombinase had been active, and CD4Cre strains were additionally backcrossed onto a *Tnfrsf1a*$^{-/-}$ background. *Ikk1*$^{fx/fx}$ *Ikk2*$^{fx/fx}$ *R26*^{REYFP} huCD2^{iCre} (IKKΔT^{CD2}), *Ikk1*$^{fx/fx}$ *R26*^{REYFP} huCD2^{iCre}, *Ikk1*$^{fx/fx}$ *Ikk2*$^{fx/fx}$ *R26*^{REYFP} CD4^{Cre} (IKKΔT^{CD4}), and *Tnfrsf1a*$^{-/-}$ *Ikk1*$^{fx/fx}$ *Ikk2*$^{fx/fx}$ *R26*^{REYFP} CD4^{Cre} (*Tnfrsf1a*$^{-/-}$ IKKΔT^{CD4}), together with F5 *Rag1*$^{-/-}$ and pLck IκB-PEST (Voll et al., 2000) mice, were bred in a conventional colony free of pathogens at the National Institute for Medical Research (London, England, UK). All mice are on a C57Bl6/J background (N5) except F5 *Rag1*$^{-/-}$ strains that are on a mixed H-2^{b} C57BL6/J/129S1/SvlmJ background. Groups of mice were treated with anti-TNF mAb (Clone XT3.11; Bio X Cell), with a 1-mg/injection delivered i.p. Controls received injections of PBS. Animal experiments were performed according to institutional guidelines and Home Office regulations.

Flow cytometry. Flow cytometric analysis was performed with 2–5 × 10^{6} thymocytes and 1–5 × 10^{6} lymph node or spleen cells. Cell concentrations of thymocytes, lymph node, and spleen cells were determined with a Scharf Instruments Casy Counter. Cells were incubated with saturating concentrations of antibodies in 100 µl of PBS containing BSA (0.1%) and 1 mM azide (PBS-BSA-azide) for 45 min at 4°C, followed by two washes in PBS-BSA-azide. Phycoerythrin (PE)–conjugated antibody against IL-7Rα, EF450-conjugated antibodies against CD4, APC-conjugated antibody against CD5, PE-Cy5– and PerCPcy5.5-conjugated antibody against TCR (H57-597), APC-Cy7– and APC-conjugated antibody against CD44, pacific orange (PO)–conjugated antibody against CD8, PE-Cy7–conjugated antibody against CD25, and PE-Cy7–conjugated antibody against HSA/CD24 were purchased from eBioscience. Cell viability was determined using LIVE/DEAD cell stain kit (Invitrogen) and active Caspase 8 was detected using CaspGLOW Red Active Caspase-8 Staining kit (BioVision Inc.), following the manufacturer's protocol. Eight-color flow cytometric staining was analyzed on a FACSCanto II or LSRFortessa X-20 (BD) instrument, and data analysis and color compensations were performed with FlowJo V9.5.3 software (Tree Star). Data are displayed on log and biexponential displays. For cell sorting, lymphocytes were incubated with the appropriate antibodies for detection of surface markers, and were then purified to >95% purity by high-speed sorting on an FAC SAria flow cytometer (BD).

In vitro culture. Thymocytes were cultured at 37°C with 5% CO_2 in RPMI-1640 (Invitrogen) supplemented with 10% (vol/vol) FBS (Invitrogen), 0.1% (vol/vol) 2-mercaptoethanol βME (Sigma-Aldrich), and 1% (vol/vol) penicillin-streptomycin (Invitrogen; RPMI-10). Recombinant TNF, BAFF, LIGHT, APRIL, TRAIL, GITRL, CD70, and TLA1 were supplemented to cultures at 100 ng/ml unless otherwise state, and were obtained from R&D Systems, with PBS used as vehicle. IKK2 inhibitor Bl605906 was used at 10 µM in DMSO vehicle. Binding of RelA from nuclear extracts of TNF-stimulated thymocytes to NF-κB oligonucleotide was determined by specific ELISA (Active Motif) according to the manufacturer's instructions.

RNA sequencing. RNA was extracted from the cells using the Isolate II RNA mini kit (Bioline). RNA-seq libraries were prepared for sequencing using Illumina Truseq RNA Library

Preparation kit (Illumina) according to the manufacturer's instructions. Samples were sequenced at the MRC National Institute for Medical Research High Throughput Sequencing Facility using an Illumina Genome Analyser IIx, and 36 bp single-end reads were obtained using the Illumina pipeline. Reads were aligned to the *Mus musculus* genome (mm9 assembly) using CLC Genomic Workbench (V5) with standard settings. Aligned reads were mapped to the RefSeq database and were normalized using the DESeq method (Anders and Huber, 2010) using Avadis NGS software V1.3.1. After normalization, reads were displayed as reads per kilobase of exon per million reads (RPKM). Data are deposited in ArrayExpress, accession nos. E-MTAB-4778 and E-MTAB-4786.

Statistics. Statistical analysis and figure preparation were performed using Graphpad Prism 6 (v6.0a). Column data compared by nonparametric unpaired two tailed Mann–Witney Student's *t* test while dose response curves were analyzed by two-way ANOVA. *, $P < 0.05$; **, $P < 0.01$; ***, $P < 0.001$; ****, $P < 0.0001$.

ACKNOWLEDGMENTS

We thank Sim Tung and Matoula Papoutsopoulou for technical assistance, the Medical Research Council National Institute for Medical Research (NIMR) Biological Services and UCL Comparative Biology Unit staff for assistance with mouse breeding, the NIMR core flow cytometry facility for performing cell sorting, and the NIMR high throughput sequencing facility.

This work was supported by the Medical Research Council UK under program code MC_PC_13055.

The authors declare no competing financial interests.

Submitted: 8 October 2015
Accepted: 27 May 2016

REFERENCES

Anders, S., and W. Huber. 2010. Differential expression analysis for sequence count data. *Genome Biol.* 11:R106. http://dx.doi.org/10.1186/gb-2010-11-10-r106

Bonizzi, G., and M. Karin. 2004. The two NF-κB activation pathways and their role in innate and adaptive immunity. *Trends Immunol.* 25:280–288. http://dx.doi.org/10.1016/j.it.2004.03.008

Brocke-Heidrich, K., B. Ge, H. Cvijic, G. Pfeifer, D. Löffler, C. Henze, T.W. McKeithan, and F. Horn. 2006. BCL3 is induced by IL-6 via Stat3 binding to intronic enhancer HS4 and represses its own transcription. *Oncogene.* 25:7297–7304. http://dx.doi.org/10.1038/sj.onc.1209711

Chen, X., J. Willette-Brown, X. Wu, Y. Hu, O.M. Howard, Y. Hu, and J.J. Oppenheim. 2015. IKKα is required for the homeostasis of regulatory T cells and for the expansion of both regulatory and effector CD4 T cells. *FASEB J.* 29:443–454. http://dx.doi.org/10.1096/fj.14-259564

Chu, Z.L., T.A. McKinsey, L. Liu, J.J. Gentry, M.H. Malim, and D.W. Ballard. 1997. Suppression of tumor necrosis factor-induced cell death by inhibitor of apoptosis c-IAP2 is under NF-κB control. *Proc. Natl. Acad. Sci. USA.* 94:10057–10062. http://dx.doi.org/10.1073/pnas.94.19.10057

Clark, K., M. Peggie, L. Plater, R.J. Sorcek, E.R. Young, J.B. Madwed, J. Hough, E.G. McIver, and P. Cohen. 2011. Novel cross-talk within the IKK family controls innate immunity. *Biochem. J.* 434:93–104. http://dx.doi.org/10.1042/BJ20101701

de Boer, J., A. Williams, G. Skavdis, N. Harker, M. Coles, M. Tolaini, T. Norton, K. Williams, K. Roderick, A.J. Potocnik, and D. Kioussis. 2003. Transgenic mice with hematopoietic and lymphoid specific expression of Cre. *Eur. J. Immunol.* 33:314–325. http://dx.doi.org/10.1002/immu.200310005

Dondelinger, Y., S. Jouan-Lanhouet, T. Divert, E. Theatre, J. Bertin, P.J. Gough, P. Giansanti, A.J. Heck, E. Dejardin, P. Vandenabeele, and M.J. Bertrand. 2015. NF-κB-independent role of IKKα/IKKβ in preventing RIPK1 kinase-dependent apoptotic and necroptotic cell death during TNF signaling. *Mol. Cell.* 60:63–76. http://dx.doi.org/10.1016/j.molcel.2015.07.032

Gareus, R., M. Huth, B. Breiden, A. Nenci, N. Rösch, I. Haase, W. Bloch, K. Sandhoff, and M. Pasparakis. 2007. Normal epidermal differentiation but impaired skin-barrier formation upon keratinocyte-restricted IKK1 ablation. *Nat. Cell Biol.* 9:461–469. http://dx.doi.org/10.1038/ncb1560

Haskill, S., A.A. Beg, S.M. Tompkins, J.S. Morris, A.D. Yurochko, A. Sampson-Johannes, K. Mondal, P. Ralph, and A.S. Baldwin Jr. 1991. Characterization of an immediate-early gene induced in adherent monocytes that encodes IκB-like activity. *Cell.* 65:1281–1289. http://dx.doi.org/10.1016/0092-8674(91)90022-Q

Hettmann, T., and J.M. Leiden. 2000. NF-kappa B is required for the positive selection of $CD8^+$ thymocytes. *J. Immunol.* 165:5004–5010. http://dx.doi.org/10.4049/jimmunol.165.9.5004

Jimi, E., I. Strickland, R.E. Voll, M. Long, and S. Ghosh. 2008. Differential role of the transcription factor NF-κB in selection and survival of $CD4^+$ and $CD8^+$ thymocytes. *Immunity.* 29:523–537. http://dx.doi.org/10.1016/j.immuni.2008.08.010

Jono, H., J.H. Lim, L.F. Chen, H. Xu, E. Trompouki, Z.K. Pan, G. Mosialos, and J.D. Li. 2004. NF-kappaB is essential for induction of CYLD, the negative regulator of NF-κB: evidence for a novel inducible autoregulatory feedback pathway. *J. Biol. Chem.* 279:36171–36174. http://dx.doi.org/10.1074/jbc.M406638200

Kreuz, S., D. Siegmund, P. Scheurich, and H. Wajant. 2001. NF-κB inducers upregulate cFLIP, a cycloheximide-sensitive inhibitor of death receptor signaling. *Mol. Cell. Biol.* 21:3964–3973. http://dx.doi.org/10.1128/MCB.21.12.3964-3973.2001

Li, Z.W., S.A. Omori, T. Labuda, M. Karin, and R.C. Rickert. 2003. IKKβ is required for peripheral B cell survival and proliferation. *J. Immunol.* 170:4630–4637. http://dx.doi.org/10.4049/jimmunol.170.9.4630

Lombardi, L., P. Ciana, C. Cappellini, D. Trecca, L. Guerrini, A. Migliazza, A.T. Maiolo, and A. Neri. 1995. Structural and functional characterization of the promoter regions of the NFKB2 gene. *Nucleic Acids Res.* 23:2328–2336. http://dx.doi.org/10.1093/nar/23.12.2328

Mahmud, S.A., L.S. Manlove, H.M. Schmitz, Y. Xing, Y. Wang, D.L. Owen, J.M. Schenkel, J.S. Boomer, J.M. Green, H. Yagita, et al. 2014. Costimulation via the tumor-necrosis factor receptor superfamily couples TCR signal strength to the thymic differentiation of regulatory T cells. *Nat. Immunol.* 15:473–481. http://dx.doi.org/10.1038/ni.2849

Micheau, O., S. Lens, O. Gaide, K. Alevizopoulos, and J. Tschopp. 2001. NF-κB signals induce the expression of c-FLIP. *Mol. Cell. Biol.* 21:5299–5305. http://dx.doi.org/10.1128/MCB.21.16.5299-5305.2001

Miller, M.L., M. Mashayekhi, L. Chen, P. Zhou, X. Liu, M. Michelotti, N. Tramontini Gunn, S. Powers, X. Zhu, C. Evaristo, et al. 2014. Basal NF-κB controls IL-7 responsiveness of quiescent naïve T cells. *Proc. Natl. Acad. Sci. USA.* 111:7397–7402. http://dx.doi.org/10.1073/pnas.1315398111

Mora, A.L., D. Chen, M. Boothby, and D.H. Rubin. 1999. Lineage-specific differences among $CD8^+$ T cells in their dependence of NF-κB/Rel signaling. *Eur. J. Immunol.* 29:2968–2980. http://dx.doi.org/10.1002/(SICI)1521-4141(199909)29:09<2968::AID-IMMU2968>3.0.CO;2-X

Saini, M., C. Sinclair, D. Marshall, M. Tolaini, S. Sakaguchi, and B. Seddon. 2010. Regulation of Zap70 expression during thymocyte development enables temporal separation of CD4 and CD8 repertoire selection at

different signaling thresholds. *Sci. Signal.* 3:ra23. http://dx.doi.org/10.1126/scisignal.2000702

Schmidt-Supprian, M., G. Courtois, J. Tian, A.J. Coyle, A. Israël, K. Rajewsky, and M. Pasparakis. 2003. Mature T cells depend on signaling through the IKK complex. *Immunity.* 19:377–389. http://dx.doi.org/10.1016/S1074-7613(03)00237-1

Schmidt-Supprian, M., J. Tian, E.P. Grant, M. Pasparakis, R. Maehr, H. Ovaa, H.L. Ploegh, A.J. Coyle, and K. Rajewsky. 2004. Differential dependence of $CD4^+CD25^+$ regulatory and natural killer-like T cells on signals leading to NF-κB activation. *Proc. Natl. Acad. Sci. USA.* 101:4566–4571. http://dx.doi.org/10.1073/pnas.0400885101

Schwenzer, R., K. Siemienski, S. Liptay, G. Schubert, N. Peters, P. Scheurich, R.M. Schmid, and H. Wajant. 1999. The human tumor necrosis factor (TNF) receptor-associated factor 1 gene (TRAF1) is up-regulated by cytokines of the TNF ligand family and modulates TNF-induced activation of NF-κB and c-Jun N-terminal kinase. *J. Biol. Chem.* 274:19368–19374. http://dx.doi.org/10.1074/jbc.274.27.19368

Senftleben, U., Z.W. Li, V. Baud, and M. Karin. 2001. IKKbeta is essential for protecting T cells from TNFα-induced apoptosis. *Immunity.* 14:217–230. http://dx.doi.org/10.1016/S1074-7613(01)00104-2

Silva, A., G. Cornish, S.C. Ley, and B. Seddon. 2014. NF-κB signaling mediates homeostatic maturation of new T cells. *Proc. Natl. Acad. Sci. USA.* 111:E846–E855. http://dx.doi.org/10.1073/pnas.1319397111

Srinivas, S., T. Watanabe, C.S. Lin, C.M. William, Y. Tanabe, T.M. Jessell, and F. Costantini. 2001. Cre reporter strains produced by targeted insertion of EYFP and ECFP into the ROSA26 locus. *BMC Dev. Biol.* 1:4. http://dx.doi.org/10.1186/1471-213X-1-4

Ten, R.M., C.V. Paya, N. Israël, O. Le Bail, M.G. Mattei, J.L. Virelizier, P. Kourilsky, and A. Israël. 1992. The characterization of the promoter of the gene encoding the p50 subunit of NF-κB indicates that it participates in its own regulation. *EMBO J.* 11:195–203.

Turner, D.J., S.M. Alaish, T. Zou, J.N. Rao, J.Y. Wang, and E.D. Strauch. 2007. Bile salts induce resistance to apoptosis through NF-κB-mediated XIAP expression. *Ann. Surg.* 245:415–425. http://dx.doi.org/10.1097/01.sla.0000236631.72698.99

Vandenabeele, P., L. Galluzzi, T. Vanden Berghe, and G. Kroemer. 2010. Molecular mechanisms of necroptosis: an ordered cellular explosion. *Nat. Rev. Mol. Cell Biol.* 11:700–714. http://dx.doi.org/10.1038/nrm2970

Voll, R.E., E. Jimi, R.J. Phillips, D.F. Barber, M. Rincon, A.C. Hayday, R.A. Flavell, and S. Ghosh. 2000. NF-κB activation by the pre-T cell receptor serves as a selective survival signal in T lymphocyte development. *Immunity.* 13:677–689. http://dx.doi.org/10.1016/S1074-7613(00)00067-4

Wang, C.Y., M.W. Mayo, R.G. Korneluk, D.V. Goeddel, and A.S. Baldwin Jr. 1998. NF-κB antiapoptosis: induction of TRAF1 and TRAF2 and c-IAP1 and c-IAP2 to suppress caspase-8 activation. *Science.* 281:1680–1683. http://dx.doi.org/10.1126/science.281.5383.1680

Yan, J., J. Xiang, Y. Lin, J. Ma, J. Zhang, H. Zhang, J. Sun, N.N. Danial, J. Liu, and A. Lin. 2013. Inactivation of BAD by IKK inhibits TNFα-induced apoptosis independently of NF-κB activation. *Cell.* 152:304–315. http://dx.doi.org/10.1016/j.cell.2012.12.021